ARTICLES
PUBLISHED ONLINE: 1 DECEMBER 2013 | DOI: 10.1038/NCLIMATE2055
nature climate change

Mid-latitude westerlies as a driver of glacier variability in monsoonal High Asia

Thomas Mölg*, Fabien Maussion and Dieter Scherer

Glaciers in High Asia store large amounts of water and are affected by climate change. Efforts to determine decadal-scale glacier change are therefore increasing, predicated on the concept that glaciers outside the northwest of the mountain system are controlled by the tropical monsoon. Here we show that the mass balance of Zhadang Glacier on the southern Tibetan Plateau, 2001–2011, was driven by mid-latitude climate as well, on the basis of high-altitude measurements and combined atmospheric–glacier modelling. Results reveal that precipitation conditions in May–June largely determine the annual mass-balance, but they are shaped by both the intensity of Indian summer monsoon onset and mid-latitude dynamics. In particular, large-scale westerly waves control the tropospheric flow strength over the Tibetan Plateau remotely. This strength alone explains 73% of interannual mass-balance variability of Zhadang Glacier, and affects May–June precipitation and summer air temperatures in many parts of High Asia's zone of monsoon influence. Thus, mid-latitude climate should be considered as a possible driver of past and future glacier changes in this zone.

Glaciers in High Asia have great potential to modify the regional hydrology[1] and to trigger natural hazards[2], and they contribute to sea-level change[3]. Moreover, they are valuable indicators of variability in the Asian monsoon[4], a major component of the global climate system. Given this importance, a number of recent studies have quantified glacier change in High Asia[2,5–8] and documented widespread glacier loss in recent decades. Only in some northwestern parts have glaciers been stable in the past decade, a behaviour termed the Pamir/Karakoram anomaly[7,8]. The typical framework used to interpret the regionally variable changes is to assume a dominant influence of the mid-latitude westerlies in the northwest of the mountain system through winter precipitation, and monsoon dominance elsewhere through summer precipitation and temperature (for example, refs 5,6). However, physically based studies that evaluate possible contributions from various large-scale circulation systems to local mass-balance controls do not yet exist.

Here we test the hypothesis that 11 years of mass-balance variability on Zhadang Glacier, located on the southern Tibetan Plateau (30° N) in the reach of monsoon influence[6], can be explained consistently by monsoon activity. The glacier is known to be affected by the Indian summer monsoon[4] (ISM), has shrunk in concert with other glaciers in the region over recent decades[9], and has been the subject of an intensive field program in recent years (Fig. 1a). It thus provides a unique case study opportunity. We focus on large-scale circulation effects, because local meteorological influences on the mass-balance (temperature and precipitation sensitivity) were investigated in a previous study[4], and were also presented in other studies of local-scale mass-balance and underlying processes in Tibet[10,11].

The data basis

Our work builds on the High Asia Reanalysis (HAR), in which a low-resolution global meteorological data set is dynamically downscaled using a numerical atmospheric model (Methods). The resultant high-resolution data are available at 30 km horizontal resolution over southern and central Asia, and at 10 km resolution over High Asia (Fig. 1a) for the period 2001–2011. HAR altitude of the grid cell containing Zhadang Glacier (5,611 m) represents the glaciated elevations, which span the range 5,516–5,983 m (Fig. 1a, inset). Therefore, we use 2-m air temperature, 2-m relative humidity, 10-m wind speed, air pressure, precipitation and cloud cover of this HAR grid cell (Supplementary Fig. 1) as direct input to a physically based glacier model[4,12], which computes the climatic mass-balance of a glacier from various mass and energy fluxes at hourly intervals (Methods). Thus, the strategy to obtain glacier-wide mass-balance on Zhadang for 2001–2011 follows the new approach of 'explicit atmospheric/mass-balance modelling': a mesoscale atmospheric model (with whatever forcing technique) is employed to model high-resolution meteorological conditions over a mountain glacier that do not require further statistical downscaling for use in a mass-balance model[13,14] (summarized in Supplementary Methods). Figure 2a–c shows that the model calculations are in very good agreement with the available measurements on Zhadang Glacier. This is discussed further in Supplementary Discussion and makes our combined HAR–mass-balance modelling system suitable for the analysis of processes that affect glacier mass.

To put the calculated mass-balance (Fig. 2d) into an independent context, global and large-scale gridded meteorological data, which are not a part of the HAR product, are area-averaged for various regions (Fig. 1a). The time series of these area-averages can be used as climate indices, which are discussed below in connection with the results. As a starting point, it is important to note that the typical ISM circulation is established between 25 May and 24 June (Fig. 1b), henceforth the 'ISM onset period'. A strong (weak) intensity of the ISM onset, that is, high (low) precipitation in the ISM region, does not always coincide with early (late) onset of the circulation (Fig. 1b), but such cases can be expected owing to internal climate variability[15]. The 'main ISM season' lasts from 25 June to as late as 19 October (Fig. 1b).

Influences of large-scale climate dynamics

The characteristics of monsoon onset are one appreciable driver of Zhadang's mass-balance. Figure 3 illustrates that strong ISM

Chair of Climatology, Technische Universität Berlin, 12165 Berlin, Germany. *e-mail: thomas.moelg@campus.tu-berlin.de

© 2014 Macmillan Publishers Limited. All rights reserved

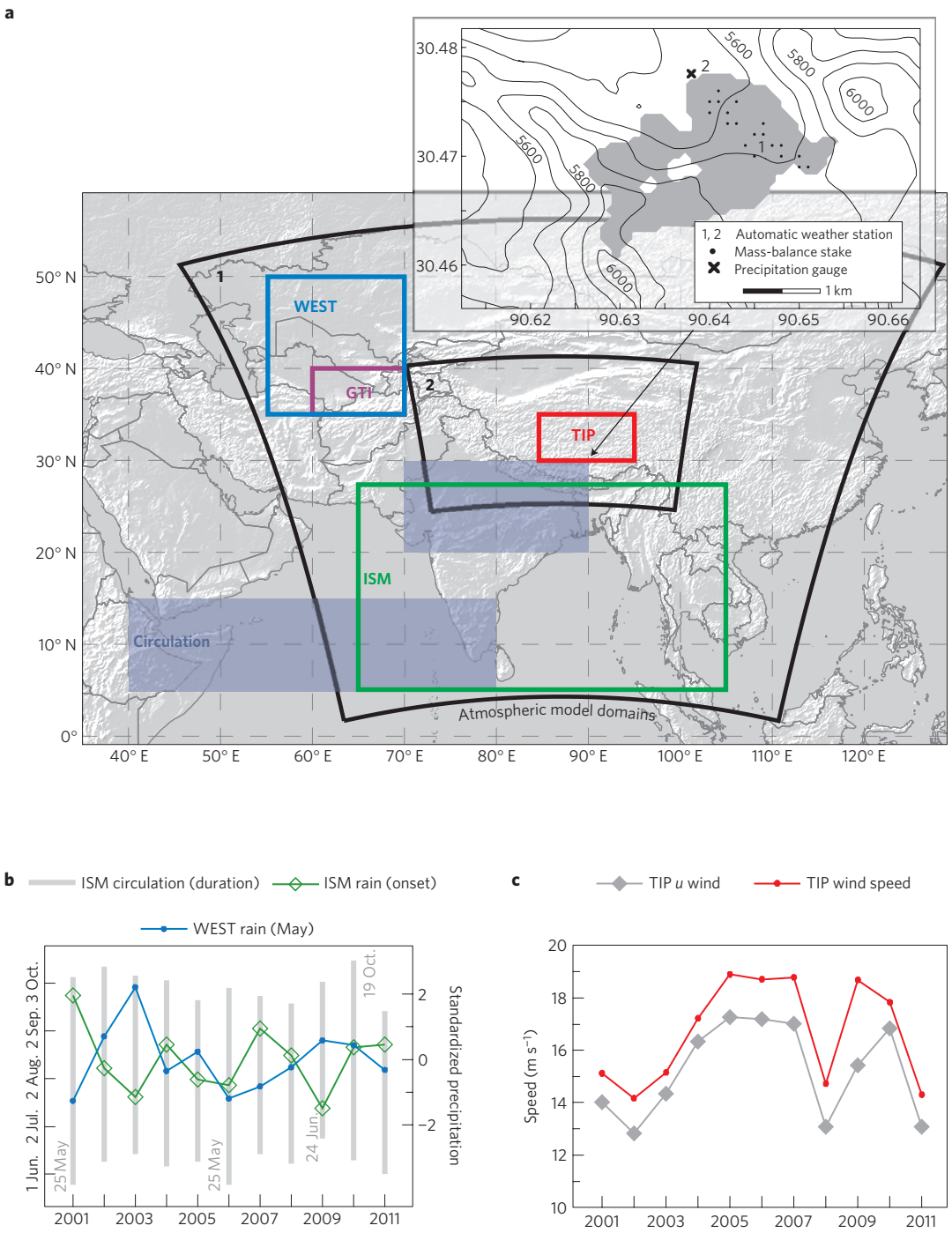

Figure 1 | Study site and indicators of large-scale dynamics. a, Atmospheric model domains (30 and 10 km horizontal resolution in domain 1 and 2, respectively) and the climate index regions: precipitation for the WEST and for the ISM region as indicators of the intensity of mid-latitude circulation and the ISM, respectively; winds at 300 hPa over the TIP region; and geopotential height at 200 hPa in the GTI region[20]; zonal wind at 850 hPa in the blue-shaded rectangles serves to determine the establishment and duration of the ISM circulation (Supplementary Methods). Data sources and areal delineations are detailed in the Methods and Supplementary Methods. The inset shows Zhadang Glacier in the mass-balance model and the measurement sites. **b**, Duration of the ISM circulation (left *y* axis; dates in the plot show earliest and latest onsets and the latest cessation) and standardized precipitation in WEST region for May and ISM region for the ISM onset period. **c**, Wind speed and zonal (*u*) wind at 300 hPa in the TIP region for the ISM onset period. A positive *u*-component means eastward flow.

onset typically coincides with higher surface accumulation, and with less surface melt and sublimation on the glacier. However, some years deviate from this relation (2002, 2003 and 2007; green symbols in Fig. 3). Only if those years are excluded from the analysis do the surface terms show a systematic (linear) dependency on ISM onset and does the monsoon influence on mass-balance become evident (Fig. 3). Subsurface melt and refreezing seem to be unrelated to variations in ISM intensity and they roughly compensate each other in all years (Fig. 3). Thus, in light of the small sublimation amounts, mass-balance variability in this season is generally controlled by surface accumulation and melt. The main underlying cause in terms of the energy balance, which also

© 2014 Macmillan Publishers Limited. All rights reserved

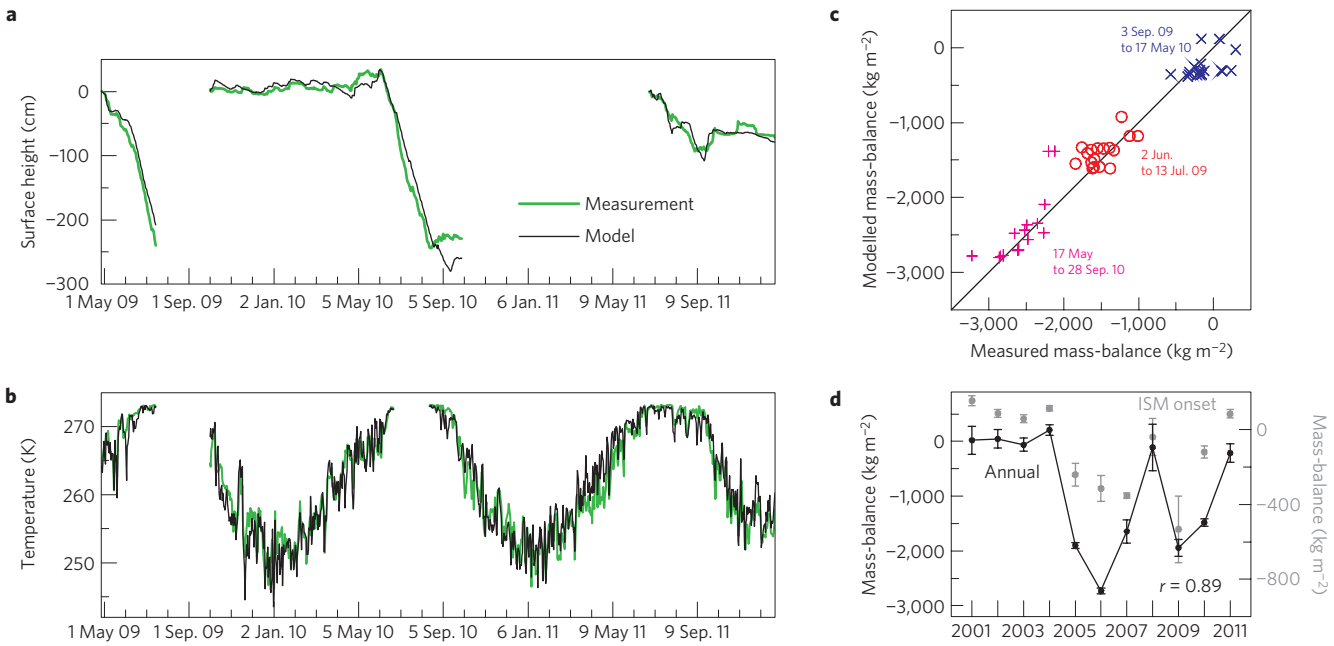

Figure 2 | *In situ* measurements and model results. a, Surface height change at AWS1 ($r = 0.98$; RMSD = 15.6 cm). **b**, Daily glacier surface temperature at AWS1 ($r = 0.96$; RMSD = 2.1 K). **c**, Mass balance for three periods at the stake locations ($r = 0.97$; RMSD = 3.1 kg m^{-2} d^{-1}). See inset of Fig. 1a for measurements sites. **d**, Modelled glacier-wide mass balance for the calendar year (left *y* axis) and the ISM onset period (right *y* axis). Error bars reflect model uncertainty as described in the Methods. All correlation coefficients are significant ($p < 0.01$).

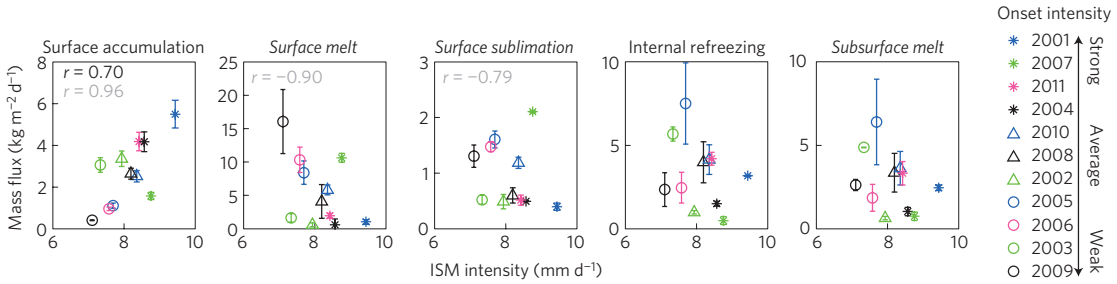

Figure 3 | Mass-balance processes and monsoon onset. Precipitation in the ISM region versus glacier-wide mass-balance components during the ISM onset period. Normal (italics) font signifies mass gain (mass loss) terms; error bars as described in the Methods. Surface deposition is very small[4] and thus not shown. The legend identifies the years and provides the order of the ISM onset intensity. Correlations are shown for all years (black) and without 2002, 2003 and 2007 (grey) if the coefficient is significant ($p < 0.05$). Note the different scaling of the *y* axes.

reflects the accumulation–albedo–melt linkage, is the variability in absorbed solar radiation (Supplementary Fig. S2). In the main ISM season, a systematic component as in Fig. 3 is not evident because intra-seasonal monsoon variability, that is, the active/break period cycle[4], does not seem to affect the local mass-balance processes. This was found for 2009–2011 previously[4] and also holds for the 2001–2011 results presented here (Supplementary Fig. 3).

The absence of a monsoon footprint on the glacier in the main ISM season may have two explanations. First, and regarding atmospheric drivers, local weather on the Tibetan Plateau begins to 'decouple' from the large-scale ISM dynamics in this season, which is discussed in detail elsewhere[4]. For example, two separate convective centres develop over the Indian Ocean and High Asia in the course of the ISM (ref. 16). Second, and from a mass-balance perspective, the conditions in the ISM onset period also leave a strong and probably dominant memory effect in the surface albedo and, thus, subsequent surface melt evolution on Zhadang (Supplementary Fig. 4). This affirms that atmospheric conditions in late spring/early summer, whatever large-scale influences operate, are pivotal for shaping the annual mass-balance. So far this was evident only for single years[4], but the high correlation in Fig. 2d corroborates this point for the decade scale. ISM dynamics clearly influence late spring–early summer climate and mass-balance response (Fig. 3), yet they cannot explain the mass-balance variability at Zhadang in all years.

Hence, what large-scale systems other than the ISM can determine local atmospheric conditions in the early monsoon season? We observe an anti-correlation of precipitation variability in the western Tien Shan (WEST) and ISM region (Fig. 1a) during spring/early summer, which indicates a 'competition' between monsoon and mid-latitude circulation. This anti-correlation is significant only if WEST leads ISM precipitation, for example by ~1 month as in Fig. 1b ($r = -0.62$; $p < 0.05$). Including this lead time makes sense, because WEST intensity is better captured in May when seasonal precipitation peaks in the WEST region[17]. An out-of-phase relationship between WEST and ISM moisture climate is also indicated by proxy records[18] and by climate dynamics studies, which recently focused on the mid-latitude circumpolar wave train[19,20] and on the interaction/bridging mechanisms[20,21]. The region of the global train index (GTI) in Fig. 1a, for example, captures such a bridge[21] (Supplementary Methods). On a larger scale, many of the dynamics studies identified the high-level

© 2014 Macmillan Publishers Limited. All rights reserved

westerly jet[22] with its core at 200–300 hPa as a crucial element connecting mid-latitude and monsoon dynamics[19–21]. Here we find implications of the jet position in the ISM onset period for Zhadang's annual glacier mass-balance (Fig. 2d and Supplementary Fig. 5): above-average mass-balance is favoured by maximum jet activity well to the north of the Tibetan Plateau (2001–2004, 2008, 2011), whereas clearly negative mass-balances coincide with frequent jet occurrences over the plateau (2007, 2010) or a curved jet axis that stretches into the western plateau (2005, 2009). Only 2006 differs from this pattern (discussed further below), so in general the jet position seems able to modify the monsoon–mass-balance relation.

First, average/weak ISM onsets (as in 2002/2003) can still coincide with high accumulation and little melt (Fig. 3), and thus above-average glacier mass-balance (Fig. 2d). High precipitation upstream in the WEST region (Fig. 1b), in combination with a northerly jet location and intensified moisture advection from the mid-latitudes (Supplementary Fig. 6), provide the likely reasons. Similar ISM and WEST conditions in 2005/2009, however, lead to negative mass-balances because the jet axis was far south over the western plateau, reducing the north–south pressure gradient and moisture import from WEST (Supplementary Fig. 7). Second, jet activity over much of the plateau as in 2007 (Supplementary Fig. 5) also seems able to limit the northward monsoon progression despite a strong ISM onset case. Hence, low glacier accumulation, abundant melt and a negative mass-balance developed in 2007 (Figs 2d and 3). Third, average WEST and ISM circulation intensities as in 2008 (Fig. 1b) may still lead to above-average mass-balance if the jet is clearly north of the plateau (Supplementary Fig. 5).

These considerations imply that the strength of the regional atmospheric flow over the Tibetan Plateau must be important for glacier mass-balance. Indeed, 300 hPa wind speed during ISM onset over the Tibetan Plateau's central part (TIP; Fig. 1c) emerges as an excellent predictor for the annual mass-balance, $r = -0.86$ ($p < 0.01$) and $r^2 = 0.73$. The relation also holds for 2006 (high wind speed, low mass-balance) despite few jet occurrences over TIP in this year (Supplementary Discussion). An understandable physical basis of the strong negative correlation is provided by cloud-resolving modelling, which showed that a weak flow favours convective cell growth[23,24]. Furthermore, the relationship of low wind speeds promoting precipitation was measured on high mountain summits[25]. This raises the question of the controls of TIP wind speed during the ISM onset period.

The main result of our teleconnection analyses is presented in Fig. 4. It shows that the correlation field of upper-level meridional winds with TIP wind speed exhibits distinct centres that originate upstream, which is characteristic of the mid-latitude wave train[19]. The wave train, furthermore, maintains close links with North Atlantic climate[19,26] and is part of a circumglobal pattern[20,26] (see further in Supplementary Discussion). The same correlation analysis using upper-level zonal winds did also not show centres in the tropical ISM zone. This result reinforces a role of the jet for glacier mass-balance because the jet acts as the wave guide[20,26] and shows the highest meridional variability in late spring[22], the key season for annual mass-balance. The result also demonstrates a major influence of the extratropical westerlies, even in the south of the Tibetan Plateau and in the monsoon season.

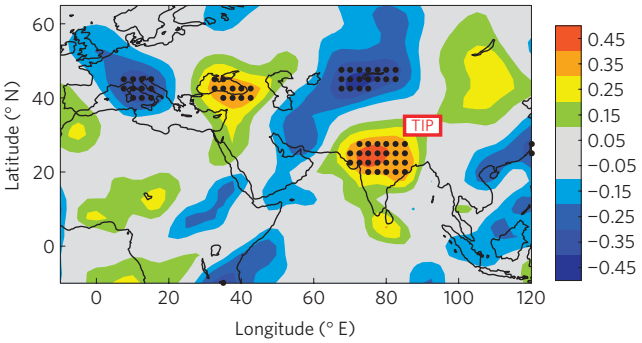

Figure 4 | Control of the atmospheric flow strength over the Tibetan Plateau. Correlation coefficient (colour scale) between area-averaged wind speed at 300 hPa over TIP and meridional winds at the same level in the ISM onset period, 1948–2011 (NCEP/NCAR reanalysis). Dots locate grid points where correlations are significant ($p < 0.01$). The structure also exists for meridional winds at 500 and 200 hPa (Supplementary Fig. 8), which indicates that the pattern is robust in the mid to high troposphere.

Regional context discussion and conclusions

Statistical tests support the causal mechanisms unravelled in this study, that is, the joint control of Zhadang's mass-balance by the extratropical and tropical circulation. WEST or ISM precipitation as a single predictor for annual mass-balance is not statistically significant (Supplementary Table 1). Both together explain 40% of the variance in annual mass-balance and approximate the 95% confidence level (Supplementary Table 1). However, this is clearly less than the 73% explained by TIP wind speed alone, and WEST and ISM precipitation as additional predictors barely increase the percentage further (Supplementary Table 1). These results underline the importance of conditions at the interface between mid-latitude and monsoon circulations, as represented by TIP wind speed. It parameterizes large-scale influences, such as advection from the WEST region and interactions between the two circulations, as well as local processes such as convective activity and water recycling[27]. Unlike ISM onset intensity (Fig. 3), TIP wind speed influences mass-balance variability in all 11 years of the record, and its link to the westerly wave train indicates a non-negligible role of mid-latitude climate.

Whether the findings for Zhadang Glacier are relevant to a wider area of High Asia is, nonetheless, another vital question. As the magnitude of accumulation on the glacier in the ISM onset period is key to the physical linkages discussed in this study, TIP wind speed should exert a strong control on precipitation in this season. Figure 5a shows that this is the case at Zhadang's location, but similarly strong controls occur in large regions of the central and southern Tibetan Plateau, and along the southern fringe of the mountain system. Most glaciers in these regions belong to the 'summer accumulation' type[10] with a distinct wet-season onset in late spring/early summer, which is substantiated by a cluster analysis of glacier regimes (Supplementary Fig. 9). This type dominates the monsoonal zone of High Asia.

However, glaciers in this zone are also sensitive to summer (June–August) air temperatures[4,10,28]. This applies to the annual mass-balance of Zhadang Glacier, which shows a high correlation with both the local 2-m summer air temperature from the HAR data ($r = -0.89$; $p < 0.01$) and the TIP-region summer air temperature at 500 hPa from the global reanalysis ($r = -0.71$; $p < 0.05$). In this vein, the significant correlation of TIP wind speed in the ISM onset period with summer air temperatures over large parts of High Asia is another intriguing result (Fig. 5b). Unravelling the physics of the flow strength–air temperature linkage, including the temporal lead effect of the flow strength, is beyond the scope of this paper. The eastward (downstream) extension of significant positive correlations on the Tibetan Plateau (Fig. 5b) could possibly indicate a contribution of advection in light of the westerly zonal flow (Fig. 1c). The opposite variability of precipitation and temperature on the plateau (Fig. 5), on the other hand, could also point to local factors such as the surface albedo/temperature feedback (driven by snow-covered area) and the turbulent heat fluxes[29]. Follow-up research should therefore consider local and non-local processes.

© 2014 Macmillan Publishers Limited. All rights reserved

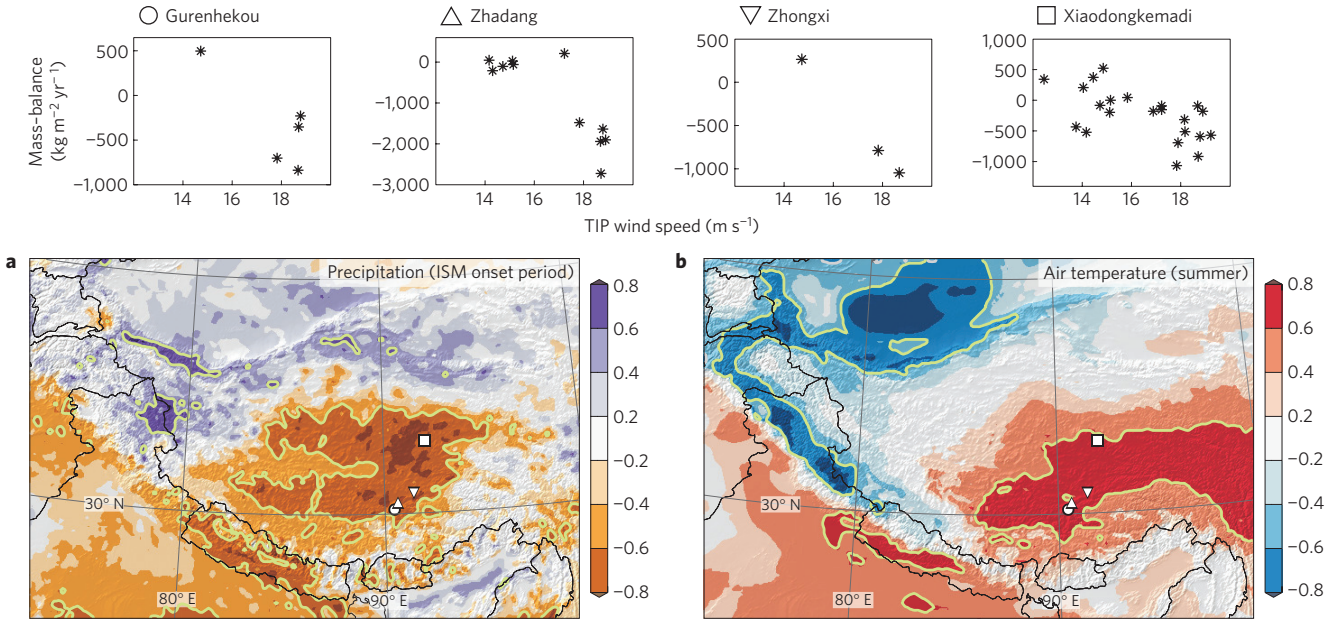

Figure 5 | Implications of the atmospheric flow strength over the Tibetan Plateau. a,**b**, Correlation coefficient (colour scales) between TIP wind speed at 300 hPa in the ISM onset period and HAR precipitation in the same period (**a**), and HAR mean 2-m air temperature in June–August, 2001–2011 (**b**). Bold pale green lines delineate statistically significant areas ($p < 0.05$); thin black lines are national borders. The top panels show annual mass-balance as a function of the TIP wind speed. In addition to Zhadang results from this study (2001–2011), direct measurements of annual mass-balance (data from ref. 6; see further in Supplementary Discussion) are shown for all available glaciers in the part where the large significant areas for precipitation and temperature intersect each other: Gurenhekou (2006–2010), Zhongxi (2008–2010) and Xiaodongkemadi (1989–2010). The glacier locations are indicated in the maps (**a**,**b**).

There are only a few annually resolved mass-balance measurements from glaciers, which allow us to complement the regional context discussion of atmospheric drivers with glaciological field data. The records that do exist are mostly short, which also complicates statistical interpretation. However, none of the available field data contradicts our Zhadang-derived finding of the inverse relationship between TIP wind speed and annual mass-balance (Fig. 5). The atmospheric links in Fig. 5a,b, moreover, exist in data from an independent global reanalysis, which suggests that these patterns are robust and have a large-scale circulation origin (Supplementary Fig. 10). Therefore, the mechanisms identified in this case study, including the contribution of mid-latitude climate to driving glacier variability, are potentially operating over a wide area of the mountain system.

The focus of our study is on mass-balance variability, but we note that the mean modelled mass-balance of Zhadang over 2001–2011 ($-891 \pm 105\,\mathrm{kg\,m^{-2}\,yr^{-1}}$; Fig. 2d) implies more mass loss, by about $500 \pm 200\,\mathrm{kg\,m^{-2}\,yr^{-1}}$, than most regional mass-balances in High Asia measured from space over a similar time period[7,30]. Furthermore, local mass-balances based on field data are often less negative[6] (for example, Fig. 5). Zhadang's estimate is close to the mean mass loss rate of South High Asia (Himalaya)[30,31], where very negative mean mass-balances of single glaciers ($< -1{,}000\,\mathrm{kg\,m^{-2}\,yr^{-1}}$; 2002–2007) were also found[31]. Peculiarities of the local environment of a glacier, as well as shortcomings in measurements and modelling, may cause the absolute differences (Supplementary Discussion). Whereas mass-balance changes in High Asia are highly heterogeneous in general[7,30], the negative mass-balance of Zhadang conforms to widespread glacier mass loss in South and East High Asia in the past decade[6,7,30].

Observations of glacier changes in High Asia are becoming increasingly important, and some of them[2,9] have emphasized the urgency of physically based studies of mass-balance controls. In this regard we combined a multi-scale, process-resolving modelling system[13] and data from field experiments to obtain results that reject the hypothesis that monsoon activity is a consistent control of Zhadang's mass-balance variability over a full decade. Only the interplay of mid-latitude and monsoon circulations provides an improved explanation. Moreover, the conditions of both systems in late spring/early summer, rather than over the entire summer season, largely control the inter-annual variability of glacier mass-balance. These insights will help to assess climate change impacts on glaciers, and to interpret contemporary changes, palaeo-extents[32] and ice core statistics[33] of glaciers in High Asia more comprehensively in future research. Our case also demonstrates how glacier-based studies can enhance understanding of the large-scale circulation variability over Asia, which underlines the need for more glacier mass-balance observations at high resolution.

Methods

HAR. Production of the HAR data employs the atmospheric model WRF (ref. 34) to downscale the Global Final Analysis data (1° horizontal resolution) to the two regional high-resolution domains shown in Fig. 1a. The atmospheric model is initialized every day and, hence, strongly constrained by the observed large-scale state of the atmosphere. This distinguishes the procedure from regional climate simulations. The atmospheric modelling strategy/settings for the HAR production were published in ref. 35. Project details and data are available at http://www.klima.tu-berlin.de/HAR.

Mass-balance modelling and uncertainty (error bars). The glacier mass-balance model[4,12] calculates the hourly glacier-wide climatic mass-balance as the sum of mass gain (accumulation of solid precipitation, surface deposition, internal refreezing) minus mass loss (surface and subsurface melt, surface sublimation) from six meteorological drivers that are provided by the HAR data for Zhadang Glacier's grid cell (Supplementary Fig. 1). During this process the mass-balance model generates the full surface energy budget (radiation balance, turbulent fluxes, energy fluxes from the ground and due to precipitation; Supplementary Fig. 2) and resolves englacial energy transfers. The distributed model uses a 60-m-resolution terrain model with the 2009 extent of Zhadang[9] (Fig. 1a, inset), and is run three times with different parameter combinations to quantify model uncertainty, as detailed in ref. 4 and summarized in Supplementary Methods.

© 2014 Macmillan Publishers Limited. All rights reserved

On-site measurements. Field measurements on Zhadang (Fig. 1a, inset) are detailed in ref. 4. The first data from automatic weather station (AWS) 1 are available on 27 April 2009, and two data gaps exist afterwards (Fig. 2a,b) due to instrument failure in the harsh environment. Ablation stake readings (Fig. 2c) were performed by Institute of Tibetan Plateau Research personnel.

Circumglobal climate data and statistical significance. Daily TRMM precipitation at 0.25° resolution, and the global NCEP/NCAR reanalysis (2.5°) for wind variables, geopotential height, and air temperature. ERA-Interim reanalysis (1°) was used for robustness checks of wind speed linkages with precipitation and temperature (Supplementary Fig. 10) and the duration of the ISM circulation (Supplementary Fig. 11). See Supplementary Methods for data sources. All significance levels reported for any data are based on a *t*-test.

Received 25 June 2013; accepted 23 October 2013; published online 1 December 2013

References

1. Kaser, G., Großhauser, M. & Marzeion, B. Contribution potential of glaciers to water availability in different climate regimes. *Proc. Natl Acad. Sci. USA* **107,** 20223–20227 (2010).
2. Bolch, T. *et al.* The state and fate of Himalayan glaciers. *Science* **336,** 310–314 (2012).
3. Marzeion, B., Jarosch, A. H. & Hofer, M. Past and future sea-level change from the surface mass balance of glaciers. *Cryosphere* **6,** 1295–1322 (2012).
4. Mölg, T., Maussion, F., Yang, W. & Scherer, D. The footprint of Asian monsoon dynamics in the mass and energy balance of a Tibetan glacier. *Cryosphere* **6,** 1445–1461 (2012).
5. Scherler, D., Bookhagen, B. & Strecker, M. R. Spatially variable response of Himalayan glaciers to climate change affected by debris cover. *Nature Geosci.* **4,** 156–159 (2011).
6. Yao, T. *et al.* Different glacier status with atmospheric circulations in Tibetan Plateau and surroundings. *Nature Clim. Change* **2,** 663–667 (2012).
7. Gardelle, J., Berthier, E., Arnaud, Y. & Kääb, A. Region-wide glacier mass balances over the Pamir–Karakoram–Himalaya during 1999–2011. *Cryosphere* **7,** 1263–1286 (2013).
8. Kääb, A., Berthier, E., Nuth, C., Gardelle, J. & Arnaud, Y. Contrasting patterns of early twenty-first-century glacier mass change in the Himalayas. *Nature* **488,** 495–498 (2012).
9. Bolch, T. *et al.* A glacier inventory for the western Nyainqentanglha Range and the Nam Co Basin, Tibet, and glacier changes 1976–2009. *Cryosphere* **4,** 419–433 (2010).
10. Fujita, K. & Ageta, Y. Effect of summer accumulation on glacier mass balance on the Tibetan Plateau revealed by mass-balance model. *J. Glaciol.* **46,** 244–252 (2000).
11. Zhang, G. *et al.* Energy and mass balance of the Zhadang Glacier surface, central Tibetan Plateau. *J. Glaciol.* **59,** 137–148 (2013).
12. Mölg, T., Cullen, N. J., Hardy, D. R., Winkler, M. & Kaser, G. Quantifying climate change in the tropical mid-troposphere over East Africa from glacier shrinkage on Kilimanjaro. *J. Clim.* **22,** 4162–4181 (2009).
13. Mölg, T. & Kaser, G. A new approach to resolving climate-cryosphere relations: Downscaling climate dynamics to glacier-scale mass and energy balance without statistical scale linking. *J. Geophys. Res.* **116,** D16101 (2011).
14. Mölg, T., Großhauser, M., Hemp, A., Hofer, M. & Marzeion, B. Limited forcing of glacier loss through land-cover change on Kilimanjaro. *Nature Clim. Change* **2,** 254–258 (2012).
15. Park, H. S., Chiang, J. C. H., Lintner, B. & Zhang, G. J. The delayed effect of major El Nino events on Indian Monsoon Rainfall. *J. Clim.* **23,** 932–946 (2010).
16. Wu, G. *et al.* Thermal controls on the Asian summer monsoon. *Sci. Rep.* **2,** 404 (2012).
17. Aizen, V. B., Aizen, E. M., Melack, J. M. & Dozier, J. Climatic and hydrologic changes in the Tien Shan, Central Asia. *J. Clim.* **10,** 1393–1404 (1997).
18. Chen, F. *et al.* Holocene moisture evolution in arid central Asia and its out-of-phase relationship with Asian monsoon history. *Quat. Sci. Rev.* **27,** 351–364 (2008).
19. Bothe, O., Fraedrich, K. & Zhu, X. Large-scale circulations and Tibetan Plateau summer drought and wetness in a high-resolution climate model. *Int. J. Climatol.* **31,** 832–846 (2011).
20. Ding, Q. & Wang, B. Circumglobal teleconnection in the northern hemisphere summer. *J. Clim.* **18,** 3483–3505 (2005).
21. Saeed, S., Müller, W. A., Hagemann, S. & Jacob, D. Circumglobal wave train and the summer monsoon over northwestern India and Pakistan: The explicit role of the surface heat low. *Clim. Dynam.* **37,** 1045–1060 (2011).
22. Schiemann, R., Lüthi, D. & Schär, C. Seasonality and interannual variability of the westerly jet in the Tibetan Plateau region. *J. Clim.* **22,** 2940–2957 (2009).
23. Kirshbaum, D. J. & Durran, D. R. Factors governing cellular convection in orographic precipitation. *J. Atmos. Sci.* **61,** 682–698 (2004).
24. Fuhrer, O. & Schär, C. Embedded cellular convection in moist flow past topography. *J. Atmos. Sci.* **62,** 2810–2828 (2005).
25. Mölg, T., Chiang, J. H. C., Gohm, A. & Cullen, N. J. Temporal precipitation variability versus altitude on a tropical high mountain: Observations and mesoscale atmospheric modeling. *Q. J. R. Meteorol. Soc.* **135,** 1439–1455 (2009).
26. Branstator, G. Circumglobal teleconnections, the jet stream waveguide, and the North Atlantic Oscillation. *J. Clim.* **15,** 1893–1910 (2002).
27. Chen, B., Xu, X. D., Yang, S. & Zhang, W. On the origin and destination of atmospheric moisture and air mass over the Tibetan Plateau. *Theoret. Appl. Climatol.* **110,** 423–435 (2012).
28. Caidong, C. & Sorteberg, A. Modelled mass balance of Xibu glacier, Tibetan Plateau: Sensitivity to climate change. *J. Glaciol.* **56,** 235–248 (2010).
29. Qian, Y., Flanner, M. G., Leung, L. R. & Wang, W. Sensitivity studies on the impacts of Tibetan Plateau snowpack pollution on the Asian hydrological cycle and monsoon climate. *Atmos. Chem. Phys.* **11,** 1929–1948 (2011).
30. Gardner, A. S. *et al.* A reconciled estimate of glacier contributions to sea level rise: 2003 to 2009. *Science* **340,** 852–857 (2013).
31. Bolch, T., Pieczonka, T. & Benn, D. I. Multi-decadal mass loss of glaciers in the Everest area (Nepal Himalaya) derived from stereo imagery. *Cryosphere* **5,** 349–358 (2011).
32. Benn, D. I. & Owen, L. A. The role of the Indian summer monsoon and the mid-latitude westerlies in Himalayan glaciation: Review and speculative discussion. *J. Geol. Soc. Lond.* **155,** 353–363 (1998).
33. Joswiak, D. R., Yao, T., Wu, G., Tian, L. & Xu, B. Ice-core evidence of westerly and monsoon moisture contributions in the central Tibetan Plateau. *J. Glaciol.* **59,** 56–66 (2013).
34. Skamarock, W. C. & Klemp, J. B. A time-split nonhydrostatic atmospheric model for weather research and forecasting applications. *J. Comput. Phys.* **227,** 3465–3485 (2008).
35. Maussion, F. *et al.* WRF simulation of a precipitation event over the Tibetan Plateau, China: An assessment using remote sensing and ground observations. *Hydrol. Earth Syst. Sci.* **15,** 1795–1817 (2011).

Acknowledgements

This work was supported by the Alexander von Humboldt Foundation and the German National Academy of Sciences (T.M.), by the German Research Foundation (DFG) Priority Programme 1372, 'Tibetan Plateau: Formation–Climate–Ecosystems' within the DynRG-TiP ('Dynamic Response of Glaciers on the Tibetan Plateau to Climate Change') project under the codes SCHE 750/4-1, SCHE 750/4-2 and SCHE 750/4-3, and by the German Federal Ministry of Education and Research (BMBF) Programme 'Central Asia–Monsoon Dynamics and Geo-Ecosystems' (CAME) within the WET project 'Variability and Trends in Water Balance Components of Benchmark Drainage Basins on the Tibetan Plateau' under the code 03G0804A. We thank M. Buchroithner, J. Curio, N. Holzer, E. Huintjes, O. Käsmacher, J. Kropáček, T. Pieczonka, J. Richters, T. Sauter, C. Schneider, B. Schröter, M. Spieß, W. Wang and the local Tibetan people for their participation in field work. We also thank T. Yao, S. Kang, W. Yang, G. Zhang and the staff of the Nam Co monitoring station from the Institute of Tibetan Plateau Research, Chinese Academy of Sciences, for leading the glaciological measurements on Zhadang and for providing ablation stake data.

Author contributions

T.M. designed the study and wrote the paper. F.M. and D.S. developed HAR and participated in field work, T.M. and F.M. conducted the numerical modelling. All authors continuously discussed the results and developed the analysis further.

Additional information

Supplementary information is available in the online version of the paper. Reprints and permissions information is available online at www.nature.com/reprints. Correspondence and requests for materials should be addressed to T.M.

Competing financial interests

The authors declare no competing financial interests.

© 2014 Macmillan Publishers Limited. All rights reserved